Increased sphingomyelin content impairs HDL biogenesis and maturation in human Niemann-Pick disease type B

Ching Yin Lee,* Alain Lesimple,† Maxime Denis,* Jérôme Vincent,* Åsmund Larsen,§ Orval Mamer,† Larbi Krimbou,* Jacques Genest,* and Michel Marcil[1,*]

Cardiovascular Genetics Laboratory,* Department of Medicine, Division of Cardiology, McGill University Health Centre/Royal Victoria Hospital, Montréal, Québec, Canada; Mass Spectrometry Unit,† McGill University, Montréal, Québec, Canada; and Department of Chemistry, University of Oslo, Oslo, Norway§

Abstract **We previously reported that human Niemann-Pick Disease type B (NPD-B) is associated with low HDL. In this study, we investigated the pathophysiology of this HDL deficiency by examining both HDL samples from NPD-B patients and nascent high density lipoprotein (LpA-I) generated by incubation of lipid-free apolipoprotein A-I (apoA-I) with NPD-B fibroblasts. Interestingly, both LpA-I and HDL isolated from patient plasma had a significant increase in sphingomyelin (SM) mass (~50–100%). Analysis of LCAT kinetics parameters (V_{max} and K_m) revealed that either LpA-I or plasma HDL from NPD-B, as well as reconstituted HDL enriched with SM, exhibited severely decreased LCAT-mediated cholesterol esterification. Importantly, we documented that SM enrichment of NPD-B LpA-I was not attributable to increased cellular mass transfer of SM or unesterified cholesterol to lipid-free apoA-I. Finally, we obtained evidence that the conditioned medium from HUVEC, THP-1, and normal fibroblasts, but not NPD-B fibroblasts, contained active secretory sphingomyelinase (S-SMase) that mediated the hydrolysis of [^{3}H]SM-labeled LpA-I and HDL$_3$. Furthermore, expression of mutant SMase (ΔR608) in CHO cells revealed that ΔR608 was synthesized normally but had defective secretion and activity. Our data suggest that defective S-SMase in NPD leads to SM enrichment of HDL that impairs LCAT-mediated nascent HDL maturation and contributes to HDL deficiency. Thus, S-SMase and LCAT may act in concert and play a crucial role in the biogenesis and maturation of nascent HDL particles.**—Lee, C. Y., A. Lesimple, M. Denis, J. Vincent, Å. Larsen, O. Mamer, L. Krimbou, J. Genest, and M. Marcil. **Increased sphingomyelin content impairs HDL biogenesis and maturation in human Niemann-Pick disease type B.** ***J. Lipid Res.*** **2006.** 47: **622–632.**

Supplementary key words high density lipoprotein • nascent LpA-I • phospholipids • sphingomyelin phosphodiesterase-1 gene • sphingomyelinase

Sphingomyelin (SM) plays an important role in the structural integrity of the cellular membranes. The constitutive degradation of SM occurs in the lysosomal compartments of the cell. Fragments of the plasma membrane containing SM targeted for degradation are endocytosed and traffic through the endosomal compartments to reach the lysosomes, where they are hydrolyzed by lysosomal sphingomyelinase. The cleaved fragments (i.e., the choline head group, the fatty acids, and the sphingoid bases) then leave the lysosome and reenter the biosynthetic pathway or can be further degraded. In Niemann-Pick type I disease, which includes types A and B (NPD-A/B), lysosomal SMase is deficient, resulting in a lysosomal accumulation of SM and a secondary increase in cholesterol (1).

Earlier studies by Tall and colleagues (2) investigated the crucial role of phospholipids (PLs) and their plasma transfer proteins in the metabolic pathway of HDL. It is well accepted that SM plays an important role in plasma lipoprotein metabolism. SM is the second most abundant PL in mammalian plasma. It appears in all major lipoproteins, where it is part of the monolayer of polar lipids and cholesterol that surrounds a core of neutral lipids. Up to 18% of total plasma PL occurs as SM, and the ratio of SM-to-phosphatidylcholine (PC) varies widely among lipoprotein subclasses (3), the lowest being in HDL. There are three major forms of HDL particles: the small lipid-poor apolipoprotein A-I (apoA-I) complex; the nascent, discoidal HDL particles containing PL and free cholesterol (FC); and the spherical α-particles in which cholesterol has been esterified by LCAT. It is commonly believed that the lipidation of apoA-I from peripheral organs involves two mechanisms: the energy-dependent ABCA1-mediated lipid

Manuscript received 7 November 2005 and in revised form 29 November 2005.

Published, JLR Papers in Press, November 30, 2005.
DOI 10.1194/jlr.M500487-JLR200

Abbreviations: apoA-I, apolipoprotein A-I; CE, cholesteryl ester; ESI-MS, electrospray ionization-mass spectrometry; FC, free cholesterol; HDL-C, high density lipoprotein-cholesterol; LpA-I, nascent apoA-I-containing particle; NPD-A/B, Niemann-Pick disease type A and B; PC, phosphatidylcholine; PL, phospholipid; rLpA-I, reconstituted apolipoprotein A-I-containing proteoliposomes; SM, sphingomyelin; SMase, sphingomyelinase; SMPD-1, sphingomyelin phosphodiesterase-1 gene; S-SMase, secretory sphingomyelinase; SR-BI, scavenger receptor class B type I; TD, Tangier disease; 2D-PAGGE, two-dimensional polyacrylamide nondenaturing gradient gel electrophoresis; 22OH/9CRA, 2.5 μg/ml 22(*R*)-hydroxycholesterol and 5 μM 9-*cis*-retinoic acid.

[1] To whom correspondence should be addressed.
e-mail: michel.marcil@mcgill.ca

efflux and the passive diffusion of PL followed by FC down a concentration gradient (4). As they circulate in the body, HDL particles remove FC from extrahepatic tissues with increased efficiency through the LCAT-mediated esterification of FC to cholesteryl esters (CEs), leading to HDL maturation in plasma (5).

Although it is well documented that SM inhibits the LCAT reaction in both discoidal and spherical reconstituted HDL in vitro, the increased SM content of HDL and its impact on the formation and maturation of HDL are poorly understood. Therefore, it is conceivable that an alteration in the SM level will have a profound effect on cellular and plasma lipid metabolism. One of the genes involved in the modulation of the SM level is sphingomyelin phosphodiesterase-1 (SMPD-1). It codes for the lysosomal SMase and secretory sphingomyelinase (S-SMase), a 70 kDa glycoprotein that hydrolyzes SM to ceramide and phosphorylcholine. Lysosomal SMase has an acidic pH optimum and is tightly associated with zinc in the cellular microenvironment. S-SMase, which has been characterized in fetal bovine serum and other cell culture media, functions at an acidic or neutral pH and requires exogenously added zinc for maximal activity (6). Although the role of S-SMase in HDL metabolism is poorly understood, Tabas (7) has documented that S-SMase has proatherogenic properties that may promote atherosclerotic vascular disease. Mutations in SMPD-1 cause the autosomal recessive disorder of NPD-A/B. We have previously reported an association between low high density lipoprotein-cholesterol (HDL-C) and mutations (ΔR608 and R441X) of SMPD-1 (8) in our NPD-B patients. However, the mechanism of their HDL-C deficiency has not been elucidated. There are several known causes of low HDL-C levels, including mutations on the ABCA1, LCAT, and apoA-I genes, as well as mutations in the lipoprotein lipase gene with increased plasma triglycerides (9). In this study, we investigated the mechanisms of low HDL-C in NPD-B by functional analysis at the cellular and plasma levels. Our results indicate that defective S-SMase in NPD-B leads to increased SM levels of both LpA-I generated in a cell culture model and plasma HDL, thus impairing the LCAT activation essential for HDL biogenesis and maturation.

MATERIALS AND METHODS

Study subjects

Normolipidemic control subjects and patients were selected from the Preventive Cardiology/Lipid Clinic of the McGill University Health Centre. The research protocol was reviewed and approved by the institutional Ethics Committee. Signed informed consent was obtained for blood sampling, DNA analysis, and fibroblast cultures. We examined two siblings (subject 303 was a 49 year old man with an HDL-C of 0.30 mmol/l, and subject 301 was a 47 year old woman with an HDL-C of 0.45 mmol/l) from a family with NPD-B. Both subjects were compound heterozygous for ΔR608 and R441X at the SMPD-1 gene, as described previously (8). Both underwent coronary artery bypass graft for severe coronary artery disease in their 40s. We also examined other siblings, as reported previously (8).

Cell culture

Cell cultures were established as described previously (10). Skin fibroblast cells from subjects 303 and 301 were used for the cellular lipid efflux experiments; cells from normal subjects and Tangier disease (TD) patients (11) were used as controls. Commercially available NPD-A/B cell lines (reference GM00112 and GM11097, respectively; Coriell Cell Repositories) were used to extend our results to other known NPD-A/B cells. HepG2, HUVEC, and THP-1 cells were cultured under standard conditions. In some cases, CHO cells were used, and they were transiently transfected with wild-type or mutant (ΔR608 and Y537H) V5/His-tagged acid SMase cDNA with Lipofectamine (Invitrogen, Carlsbad, CA) according to the manufacturer's instructions. The β-galactosidase cDNA (pCMVb) was co-transfected to control the transfection efficiency. Mutagenesis of the wild-type acid pcDNA3.1-SMPD1/GS (Invitrogen) was performed with the Quickchange II Mutagenesis kit (Stratagene, La Jolla, CA). The authenticity of all mutants was confirmed by nucleotide sequencing.

Western blot

In transient transfection experiments, cell lysates were harvested 24 h after transfection and prepared with lysis buffer (150 mM NaCl, 50 mM Tris-HCl, and 1% Triton X-100, pH 8.0). Conditioned medium was collected, spun at 800 *g* for 15 min to pellet any contaminating cells, and concentrated down to <1 ml using a Centriprep 30 concentrator (Amicon, Beverly, MA). Cell lysates or concentrated medium were boiled in loading buffer and directly loaded on SDS-10% Tris-glycine-PAGE gels after normalization with the transfection efficiency. Gels were then electrotransferred to nitrocellulose for immunoblotting. Blots were blocked with 5% dry milk and incubated with mouse anti-V5 primary antibodies (Invitrogen) and horseradish peroxidase-conjugated rabbit anti-mouse secondary antibodies (Amersham Biosciences, Piscataway, NJ). Finally, the blots were soaked in chemiluminescence reagent (Pierce, Rockford, IL) and exposed to Omat-Blue X-ray films.

Iodination of human plasma apoA-I

Purified plasma apoA-I (Biodesign, Saco, MA) was resolubilized in 4 M guanidine HCl and dialyzed extensively against PBS buffer. Freshly resolubilized apoA-I was iodinated with [^{125}I] iodine by Iodo-Gen® (Pierce) to a specific activity of 800–1,500 cpm/ng apoA-I and used within 48 h.

Preparation of LpA-I particles

For LCAT assay, nascent high density lipoprotein (LpA-I) was generated in vitro during a 24 h incubation of 10 μg/ml ^{125}I-apoA-I onto a 150 mm dish of fibroblasts that had been sequentially loaded with 20 μg/ml LDL and 10 μCi/ml [^{3}H]FC. During a 24 h equilibration period before the apoA-I incubation, cells were stimulated with 2.5 μg/ml 22(*R*)-hydroxycholesterol and 5 μM 9-cis-retinoic acid (22OH/9CRA) for 20 h. Lipid-free ^{125}I-apoA-I was removed from the conditioned (serum-free) medium by size-exclusion centrifugation (Amicon Ultra 15, MWCO 50,000; Millipore, Billerica, MA). Concentrated medium was washed five times in the same filter with 15 ml of PBS containing a protease inhibitor cocktail (Roche Diagnostics, Indianapolis, IN) and was further dialyzed for 16 h at 4°C using a dialysis membrane with a molecular weight cutoff of 50,000 to remove any residual lipid-free apoA-I (12). The concentrations of purified LpA-I particles were estimated from their specific activities. For mass spectrometry analysis, LpA-I particles were generated by a similar method (12) except that 20 μg/ml unlabeled apoA-I was used.

Preparation of reconstituted HDL particles

Discoidal reconstituted apolipoprotein A-I-containing proteoliposomes (rLpA-I) were prepared by sodium cholate dialysis methods as described by Jonas, Steinmetz, and Churgay (13). Two distinct rLpA-I particles were formed, apoA-I/POPC/cholesterol and apoA-I/POPC/SM/FC, using molar ratios of 1:100:5 and 1:100:200:5, respectively. Approximately 62 nCi of [^{3}H]FC was added per nanomole of unlabeled FC, and an equimolar amount of sodium cholate to POPC was used to solubilize the lipids during preparation. Lipid-free apoA-I was removed from the preparation as described above. The integrity of isolated rLpA-I particles was verified by analysis with two-dimensional polyacrylamide nondenaturing gradient gel electrophoresis (2D-PAGGE), as described previously (12).

Lipoprotein isolation and reconstituted LDL

Human plasma LDL ($1.019 < d < 1.063$) and HDL ($1.090 < d < 1.210$) were isolated from fresh plasma by sequential ultracentrifugation using potassium bromide for density adjustments (14). The apoA-I concentration of purified plasma HDL was measured and used to normalize the PL quantitation. Purified plasma LDL was labeled with [1α,2α(n)-^{3}H]cholesteryl oleate (CE) (Amersham, Piscataway, NJ) by the method of Roberts et al. (15) using the lipoprotein-free fraction ($d > 1.215$) of fresh human serum as the source of CE transfer protein. The labeled LDL was then reisolated by ultracentrifugation. The physical characteristics of the reconstituted LDL have been assessed by a 0.75% agarose gel stained by Polygon Lipostain (Beckman Coulter, Fullerton, CA).

PL efflux

Fibroblasts used in all lipid efflux experiments were loaded with 20 μg/ml LDL and 20 μg/ml cholesterol to enhance intracellular SM and cholesterol storage (16). Lipid efflux was determined as the percentage of ^{3}H radioactivity in the medium over the total ^{3}H radioactivity (^{3}H in medium + ^{3}H in cells). In PL efflux experiments, cells were labeled with [^{3}H]choline as described previously (16). PL from the efflux medium and cells were extracted with chloroform-methanol (2:1, v/v) and hexane-isopropanol (3:2, v/v), respectively, and were fractionated by TLC developed in a chloroform-methanol-water (65:35:4, v/v/v) mixture. SM and PC were scraped from the TLC plates and counted directly. Individual lipid classes were identified from their comigration with pure standards of major cellular and plasma PL.

Lysosome-targeted LDL-derived cholesterol efflux

For LDL-[^{3}H]CE efflux analysis, 75% confluent fibroblasts were grown overnight in lipoprotein-deficient serum to upregulate the LDL receptor. The cells were then loaded with 20 μg/ml reconstituted LDL-[^{3}H]CE for 24 h, followed by 20 μg/ml unlabeled FC loading that was allowed to equilibrate for an additional 24 h. Finally, labeled cells were incubated in medium containing purified apoA-I as the lipid acceptor (10 μg/ml) for 24 h. Efflux medium and cell lysate were harvested, and their radioactivity was counted. To further examine the lipid efflux ability of the NPD-B fibroblasts under excess SM feeding conditions, they were also treated with exogenous SM specifically targeted to the lysosomal compartment through receptor-mediated endocytosis of purified SM-labeled LDL (16), prepared with SM/PC (158 nmol/33 nmol) liposomes. For filipin staining, cells were treated additionally with 5 μM lovastatin (Sigma Chemical, St. Louis, MO) to decrease endogenous cholesterol synthesis before the 24 h efflux with 10 μg/ml apoA-I.

Lipid mass quantitation

Cellular cholesterol mass was measured with a commercially available enzymatic kit (Infinity Cholesterol Measurement kit; Sigma Chemical). For PL mass analysis of cellular extracts, cells were lysed with 0.1 N sodium hydroxide and cellular lipids were extracted with chloroform-methanol (2:1, v/v). PC and SM were separated by TLC, scraped, and measured using the phosphorus method (17). The cellular protein concentration was measured using the Lowry method and was used to normalize the lipid quantitation. For PL mass analysis on HDL samples, electrospray ionization-mass spectrometry (ESI-MS) was used instead because of its higher sensitivity and unmatched accuracy for our highly purified analytes of limited quantity (18). ESI-MS analysis was carried out in positive and negative ion modes using a Micromass Quattro II triple quadrupole mass spectrometer equipped with an electrospray source, as we have reported previously (18){22}. Quantitation of the analyte species was performed by ESI-MS by comparisons of individual ion peak intensity with internal standards of known amounts (i.e., C19:0/C19:0 PC and N17:0 SM) followed by correction for the natural abundance of heavy isotope substitution.

Lecithin:cholesterol acyltransferase assay

Carboxyl-terminal histidine-tagged human recombinant lecithin:cholesterol acyltransferase was a gift from Dr. John Parks (Wake Forest University School of Medicine, Winston-Salem, NC). Cholesterol esterification experiments were conducted as described previously (19). Briefly, equivalent amounts of either normal or NPD-B LpA-I were reacted with 50–500 ng of LCAT for 1 h at 37°C in a 200 μl reaction mixture consisting of 1.5 mg of fatty acid-free BSA, 5 mM β-mercaptoethanol, and Tris buffer (10 mM Tris, 150 mM NaCl, 1 mM EDTA, and 1 mM NaN_3, pH 8.0). In separate experiments, rLpA-I (POPC or POPC/SM reconstituted) was reacted with LCAT as described above. Under these conditions, initial rates were estimated with minimal substrate conversion. For plasma HDL purified from normal and NPD-B subjects, both the fractional esterification rate of cholesterol and LCAT activity within the samples were determined using a modified procedure as described previously (20).

SMase assay

For the SMase assay with purified normal HDL_3 and LpA-I, labeling with [^{3}H]SM and the activity assay were performed as described previously by Jiang and colleagues (21). Briefly, 50–65 μg of HDL-[^{3}H]SM and 20 μg of normal LpA-I were incubated with 0–200 μl of concentrated conditioned medium collected from HUVEC, THP-1, or NBD-B fibroblasts in the presence or absence of 0.1 mM $ZnCl_2$. Both LpA-I and HDL-[^{3}H]SM hydrolysis were assayed by measuring the quantity of [^{3}H]phosphorylcholine cleaved and liberated from [^{3}H]SM. For the SMase assay with samples generated from the overexpression system, the activity was assessed by the scintillation proximity assay (Amersham Biosciences, Piscataway, NJ). Briefly, each 100 μl of assay mixture consisted of up to 40 μl of sample (cell lysates or conditioned medium), 0.1 M sodium acetate assay buffer, pH 5.0, with or without 0.1 M Zn^{2+}, and 0.625 pmol of [^{3}H]biotinylated SM substrate. The assay mixtures were incubated at 37°C for 1 h, and the reactions were stopped by the addition of streptavidin-scintillation beads. Only nonhydrolyzed [^{3}H]SM could be precipitated by the beads and detected by the β-counter; thus,

the cpm measured was inversely related to the amount of SM being hydrolyzed.

Statistical analysis

All experiments were done in triplicate, and the results are expressed as means ± SD. All other statistical analysis was calculated with GraphPad Prism 4.0 software (San Diego, CA).

RESULTS

NPD-B patients and control subjects

We have previously described kindred NPD-B subjects (8). Subject 303 is a 49 year old man who was admitted to a pediatric hospital in 1955 at the age of 3 years for pulmonary infiltration and hepatosplenomegaly. He underwent a splenectomy and showed normal intellectual development. A diagnosis of NPD-B was made on the basis of lipid-laden histiocytes found in the spleen and in a cervical lymph node. His 47 year old sister, subject 301, was also diagnosed as having NPD-B on the basis of splenomegaly. In addition, both of them were diagnosed as having severe coronary artery disease and both underwent coronary artery bypass in their 40s. They were referred to our clinic for evaluation of an abnormal lipoprotein profile with a marked decrease in plasma HDL-C level (subject 303 had an HDL-C of 0.30 mmol/l, and subject 301 had an HDL-C of 0.45 mmol/l). We previously found that both subjects were compound heterozygous for mutations ΔR608 and R441X of the SMPD-1 gene (8). Other subjects in the kindred were heterozygote for either the ΔR608 or R441X mutation, but none of the family members, other than 301 and 303, demonstrated significant medical problems related to splenomegaly or pulmonary infiltrates (8). Control subjects used for this study were normolipidemic individuals selected from both sexes and from different age groups (**Table 1**).

Increased levels of SM in nascent HDL generated from NPD-B fibroblasts (LpA-I) and isolated from NPD-B plasma

We previously reported that SM content was significantly increased in LpA-I particles generated by incubation of lipid-free apoA-I with NPD-B fibroblasts (22). In this experiment, only the major SM and PC species were considered for the absolute quantitation, as we have reported previously (18). Compared with normal fibroblasts, LpA-I particles generated by incubation of lipid-free apoA-I with NPD-B fibroblasts had an average increase of ~50% in SM levels (**Table 2**). Because PC levels in the lipidated apoA-I particles from NPD-B cells were only slightly higher than those of controls, there was a 17–42% increase in the SM/PC ratio. To rule out the possibility that the increased SM content in NPD-B LpA-I was not attributable to LDL loading or to an artifactual retention of SM in the cells, both normal and NPD-B fibroblasts were stimulated with 22OH/9CRA to upregulate ABCA1 levels before the apoA-I incubation. Stimulation of cells resulted in a 50–100% increase in the SM and PC contents of LpA-I generated from both normal and NPD-B cells compared with unstimulated cells (Table 2). In parallel, glyburide, an inactivator of ABCA1 transporter activity, decreased the SM content of LpA-I by >75% in both NPD-B and normal fibroblasts (data not shown). Importantly, the increased SM content of NPD-B LpA-I was preserved upon ABCA1 upregulation. This supports the specificity of SM enrichment in NPD-B LpA-I particles.

We next sought to assess the size and charge distribution of these SM-enriched LpA-I particles with 2D-PAGGE analysis. As shown in **Fig. 1** (upper panels), the majority of LpA-I generated by both NPD-B and normal fibroblasts after 24 h of incubation had α-electrophoretic mobility, with a particle sizes ranging from 9 to 20 nm. In separate experiments, we observed that short incubation periods (<2 h) generated only α-LpA-I particles; no detectable preβ$_1$-LpA-I particle formation was observed in stimulated

TABLE 1. SM and PC quantitation of plasma HDL particles from NPD-B and control subjects

Variable	Control 1	Control 2	Control 3	Control 4	Subject 301	Subject 303
Sex	Male	Male	Female	Female	Female	Male
Age (years)	28	45	26	44	47	49
Plasma LDL-cholesterol (mmol/l)	2.75	2.45	2.60	2.72	3.96	n.a.
Plasma HDL-cholesterol (mmol/l)	1.08	0.89	1.40	1.25	0.45	0.30
Plasma apoA-I (g/l)	1.22	1.09	1.48	1.35	0.90	0.48
SM in HDL (pmol/μg apoA-I)	30.7 ± 0.6	33.4 ± 0.9	33.6 ± 0.4	32.3 ± 0.4	59.0 ± 4.7[a]	67.8 ± 6.4[a]
PC in HDL (pmol/μg apoA-I)	400 ± 21	392 ± 27	345 ± 25	394 ± 29	652 ± 84[b]	929 ± 36[a]
SM/PC in HDL	0.08	0.09	0.10	0.08	0.09	0.07

apoA-I, apolipoprotein A-I; n.d., not determined; NPD-B, Niemann-Pick disease type B; PC, phosphatidylcholine; SM, sphingomyelin. Only the major SM and PC species were accounted for in the quantitation; they included N16:0 SM, C16:0/C18:2 PC, C16:0/C18:1 PC, C16:0/C20:4 PC, C18:2/C18:2 PC, C18:1/C18:2 PC, C16:0/C20:3 PC, C18:0/C18:2 PC, C18:1/C18:1 PC, and C16:0/C20:2 PC. The absolute quantities of SM and PC were calculated from the ion intensities obtained in electrospray ionization-mass spectrometry (ESI-MS) as described in Materials and Methods. Each value represents the mean ± SD of three preparations.

[a] $P < 0.001$, compared with the average of control samples.

[b] $P < 0.01$, compared with the average of control samples.

TABLE 2. SM and PC quantitation of nascent apoA-I-containing particles generated by incubation of lipid-free apoA-I with normal and NPD-B fibroblasts

	Control 1		Control 2		Subject 301		Subject 303	
SM or PC	−	+	−	+	−	+	−	+
	pmol/μg apoA-I/mg cell proteins							
SM	7.86 ± 0.46	13.8 ± 0.4	7.88 ± 0.76	12.6 ± 0.4	11.6 ± 0.2[a]	24.1 ± 0.02[a]	11.8 ± 1.8[b]	21.2 ± 1.2[a]
PC	63.6 ± 5.4	102 ± 1	63.4 ± 4.5	95.5 ± 6.1	67.8 ± 5.0[c]	112 ± 2[d]	83.4 ± 8.2[b]	134 ± 7[e]
SM/PC	0.12	0.14	0.12	0.13	0.17	0.21	0.14	0.16

Only the major SM and PC species were accounted for in the quantitation; they included N16:0 SM, C16:0/16:0 PC, C16:0/C18:2 PC, C16:1/C18:1 PC, C16:0/C18:1 PC, C18:0/C18:2 PC, C18:1/C18:1 PC, and C18:0/C181 PC. The absolute quantities of SM and PC were calculated from the ion intensities obtained in ESI-MS as described in Materials and Methods. Each value represents the mean ± SD of three preparations. Plus and minus signs refer to the presence and absence of 2.5 μg/ml 22(*R*)-hydroxycholesterol and 5 μM 9-*cis*-retinoic acid.

[a] $P < 0.001$, compared with the average of control samples.
[b] $P < 0.05$, compared with the average of control samples.
[c] $P > 0.1$, compared with the average of control samples.
[d] $P < 0.01$, compared with the average of control samples.
[e] $P < 0.005$, compared with the average of control samples.

fibroblasts (data not shown), consistent with our previous finding that fibroblasts did not form preβ$_1$-LpA-I particles (12). In contrast, incubation of ^{125}I-labeled lipid-free apoA-I with HepG2 generated both preβ$_1$-LpA-I and α-LpA-I. Interestingly, rLpA-I particles reconstituted with POPC alone or with POPC/SM exhibited preβ-electrophoretic mobility, with particle sizes of 10–13 nm (data not shown). Of note, the increased SM contents in both NPD-B LpA-I and

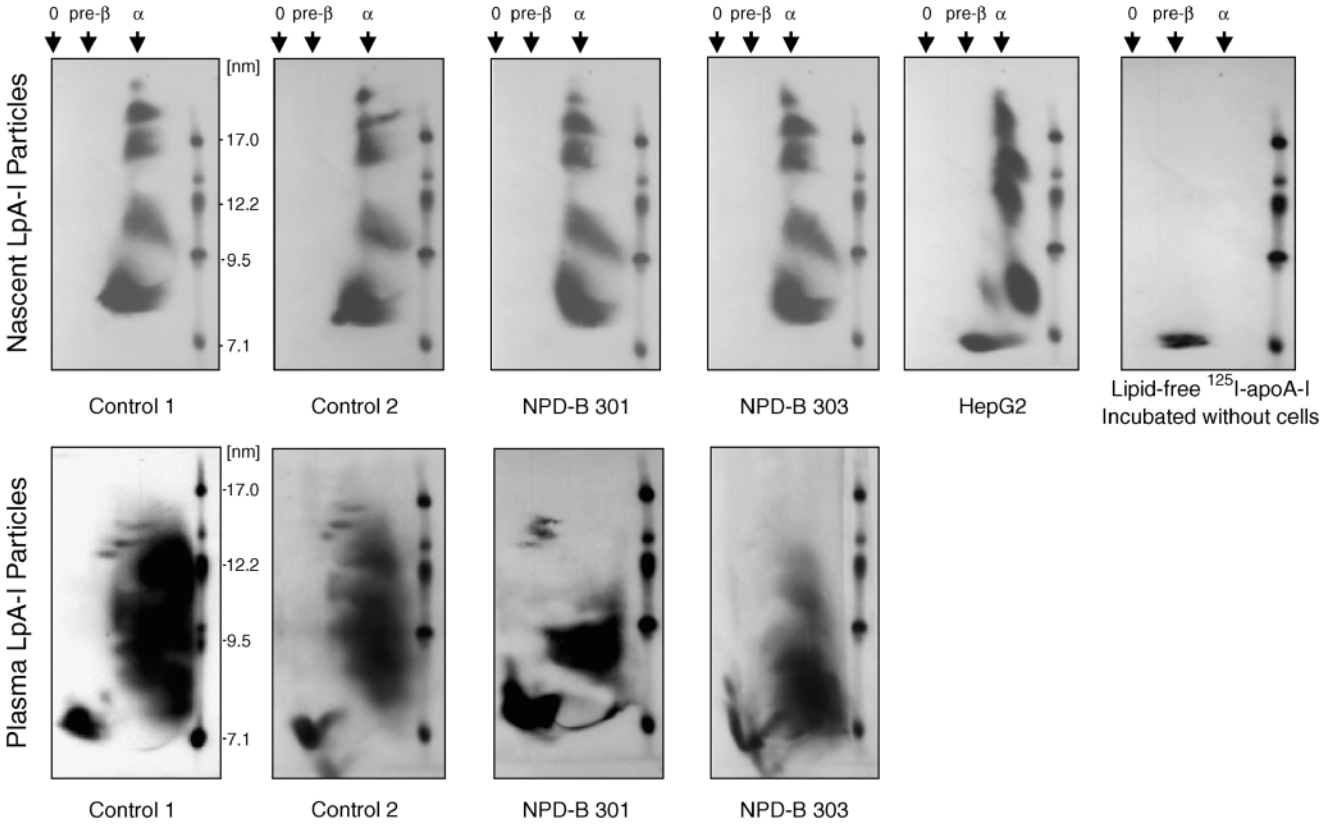

Fig. 1. Analysis of nascent high density lipoprotein (LpA-I) and plasma HDL particles from Niemann-Pick disease type B (NPD-B) subjects by two-dimensional polyacrylamide nondenaturing gradient gel electrophoresis (2D-PAGGE). In the upper panels, normal fibroblasts, NPD-B fibroblasts, or HepG2 cells in 150 mm diameter dishes were loaded with 20 μg/ml LDL, 10 μCi/ml [^{3}H]free cholesterol (FC), and 20 μg/ml cholesterol each for 24 h. During a 24 h equilibration period, cells were stimulated with 2.5 μg/ml 22(*R*)-hydroxycholesterol and 5 μM 9-*cis*-retinoic acid for 20 h. The cells were incubated with 20 μg/ml ^{125}I-apolipoprotein A-I (apoA-I) for 24 h at 37°C. Lipid-free ^{125}I-apoA-I was removed from the medium by ultrafiltration followed by dialysis, as described in Materials and Methods. Lipid-free ^{125}I-apoA-I incubated with HepG2 was used to show the presence of preβ$_1$-LpA-I particles, whereas those incubated in DMEM without cells were used as a negative control. Samples were separated by 2D-PAGGE, and ^{125}I-apoA-I was detected directly by autoradiography using Kodak XAR-2 film. Molecular size markers are shown. These same LpA-I particles generated by normal and NPD-B fibroblasts were also used for LCAT-mediated cholesterol esterification. In the lower panels, plasma from two normolipidemic and NPD-B subjects (100 μl) were separated by 2D-PAGGE, and apoA-I was detected by an anti-apoA-I antibody. Molecular size markers are shown.

SM-enriched rLpA-I affected neither the charge nor the size of these particles (23). At the same time, analysis of plasma apoA-I-containing particles from NPD-B subjects revealed a nearly complete absence of larger HDL particles in NPD-B (**Fig. 1**, lower panels). To extrapolate the relevance of these biological changes to in vivo models, we examined the HDL ($1.090 < d < 1.210$) isolated from the plasma of NPD-B patients. Similar to the LpA-I generated by NPD-B fibroblasts, our quantitative ESI-MS analysis revealed an average increase of >80% in SM level in NPD-B plasma HDL (Table 1). Interestingly, we observed an equivalent increase (average increase of >70%) in PC levels. Therefore, the overall SM/PC ratio in the NPD-B plasma HDL was not increased, as observed in the LpA-I generated in vitro. The cause of this disparity is unknown at present, but it may be attributable to PL transfer proteins involved in HDL remodeling in vivo.

Decreased cholesterol esterification rate in nascent HDL generated from NPD-B fibroblasts and isolated from NPD-B plasma

It has been proposed that the SM content in HDL is critically important because any change in lipoprotein PL composition affects the structural integrity and stability of the lipoprotein as well as its ability to interact with LCAT (24–26). HDL particles are the preferred LCAT substrate, and their reactivity varies as a function of their lipid and protein composition, nascent HDL being the most reactive. To assess the underlying impact of the increased SM content on HDL metabolism, we studied the cholesterol esterification of our two types of HDL analytes (LpA-I generated from fibroblasts and HDL purified from plasma). Initial velocities (**Table 3**) were estimated with less than ~15% substrate conversion to avoid conditions in which the substrate concentration would become rate-limiting. We observed a significant decrease in V_{max} of the LCAT reaction with NPD-B LpA-I compared with normal LpA-I, whereas estimation of K_m from double-reciprocal plots of initial velocities as a function of substrate concentration showed a 3- to 4-fold increase in the apparent K_m for NPD-B LpA-I (NPD-B 303 and NPD-B 301). Consequently, the catalytic efficiency of LCAT (V_{max}/K_m) was decreased dramatically for these nascent particles. Similarly, the catalytic efficiency of LCAT was severely decreased for rLpA-I particles enriched with SM (Table 3). As a negative control, α-LpA-I generated with apoA-I mutant Δ122–165 was used, and no significant esterification was detected (data not shown). In the case of plasma HDL, we observed a 4-fold decrease in the fractional esterification rate of HDL cholesterol in the samples from the two NPD-B patients (NPD-B 301 and NPD-B 303) (**Fig. 2**), consistent with our previous finding that FC/CE ratios were significantly increased in NPD-B HDL compared with normal control subjects (8). As controls, we assessed LCAT activity in normal and NPD-B plasma HDL by exogenous substrate LCAT assay using [^{3}H]FC-labeled reconstituted HDL and observed no significant differences between the two (data not shown). The observed decrease in esterification by LCAT, an important step in the HDL maturation process, was consistent with our 2D-PAGGE analysis of plasma apoA-I-containing particles from the two NPD-B subjects, which showed the complete absence of larger particles in the HDL_2 range (Fig. 1, lower panels).

TABLE 3. Effect of nascent and reconstituted LpA-I SM content on LCAT kinetic parameters

HDL Particles	Size[a]	Apparent V_{max}	Apparent K_m	V_{max}/K_m
	nm	*pmol CE/h*	*μM*	*nmol CE/h/μM*
Nascent LpA-I	9–20	1.2 ± 0.08[b]	0.25 ± 0.04[b]	4.80
Normal (n = 2)				
NPD-B 301	9–20	0.4 ± 0.06[b]	0.95 ± 0.07[b]	0.42
NPD-B 303	9–20	0.6 ± 0.05[b]	0.70 ± 0.03[b]	0.85
rLpA-I				
POPC	10–13	6.5 ± 0.6	0.80 ± 0.06	8.20
POPC/SM	10–13	2.4 ± 0.3	7.50 ± 1.30	0.35

CE, cholesteryl ester; LpA-I, nascent high density lipoprotein; rLpA-I, reconstituted apolipoprotein A-I-containing proteoliposomes. ApoA-I concentrations of LpA-I and reconstituted LpA-I (rLpA-I) were estimated from the initial specific activity of ^{125}I-apoA-I. Kinetic data were obtained using GraphPad Prism 4.0 software. Normal and NPD-B LpA-I as well as rLpA-I particles were prepared as described in Materials and Methods. The values are means ± SD of triplicate measures.

[a] Particle size distribution was estimated from the two-dimensional polyacrylamide nondenaturing gradient gel electrophoresis separation of HDL particles.

[b] $P < 0.001$, normal LpA-I compared with NPD-B 301 and NPD-B 303 LpA-I.

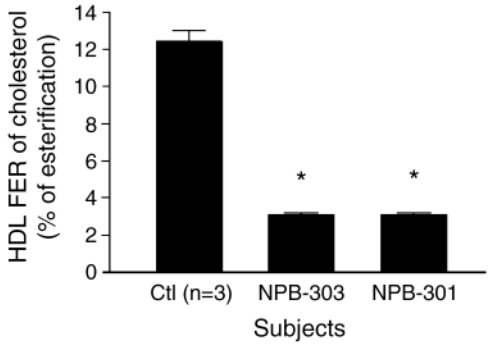

Fig. 2. Fractional esterification rate (FER) of HDL isolated from plasma of normolipidemic and NPD-B subjects. Equivalent amounts of apoA-I-containing HDL from normolipidemic [control (Ctl; n = 3)] and NPD-B subjects were labeled with [^{3}H]FC, and the fractional esterification rate of cholesterol was determined as described in Materials and Methods. Values represent means ± SD from triplicate wells. * $P < 0.001$.

Normal PL and LDL-derived cholesterol efflux in NPD-B fibroblasts

Because of the SM content increase in both LpA-I and plasma HDL in NPD-B, we asked whether the cellular mass transfer of PL could be increased in NPD-B fibroblasts. As shown in **Fig. 3**, both SM and PC efflux to lipid-free apoA-I (10 μg/ml) for 24 h (expressed as a percentage of total) was normal in NPD-B fibroblasts. TD fibroblasts, previously shown to have defective cholesterol and PL effluxes as a result of the mutation in the ABCA1 gene, were used as

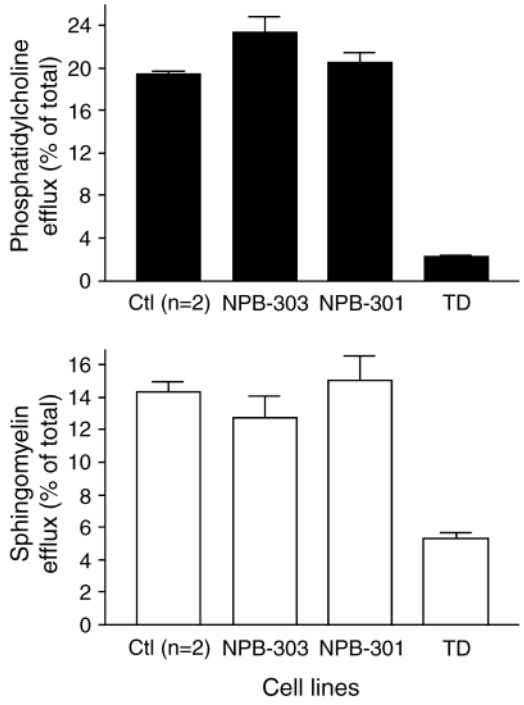

Fig. 3. Phospholipid (PL) efflux from normal and NPD-B fibroblasts. Cells were treated with [^{3}H]choline in lipoprotein-deficient serum (LPDS) for 2 days, followed by 20 μg/ml LDL for 24 h and 20 μg/ml cholesterol for another 24 h. After a subsequent 24 h equilibrium, cells were incubated with 10 μg/ml apoA-I for 24 h. PLs in the medium were extracted with chloroform-methanol (2:1, v/v), and cellular lipids were extracted with hexane-isopropanol (3:2, v/v). Lipids were then separated by TLC and scraped and counted for radioactivity. Sphingomyelin (SM; A) and phosphatidylcholine (PC; B) efflux was determined as described in Materials and Methods. Values represent means ± SD from triplicate wells. Ctl, control; TD, Tangier disease.

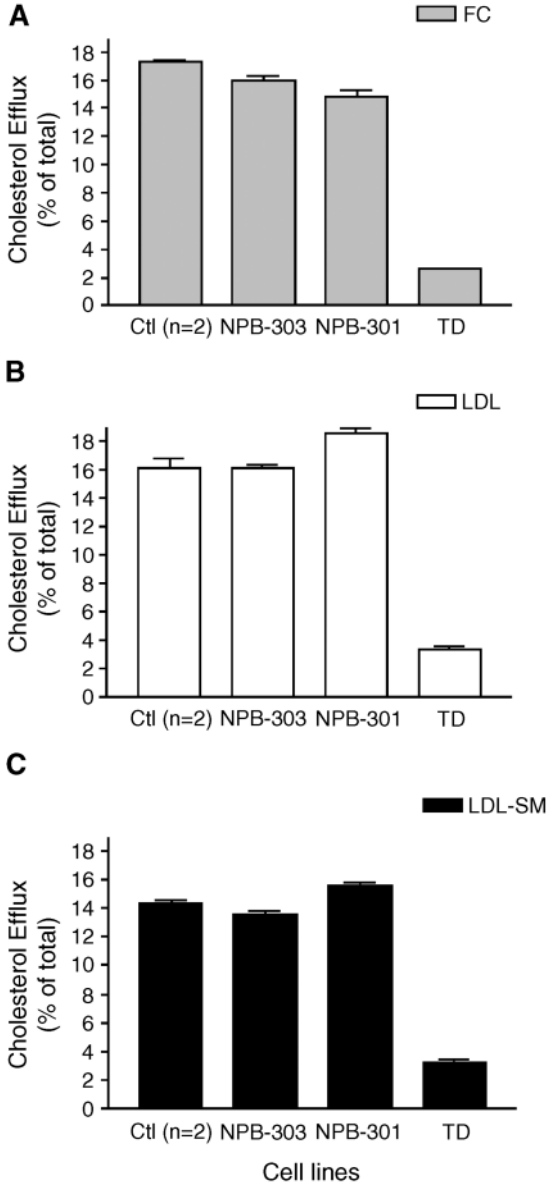

Fig. 4. Cholesterol efflux from normal and NPD-B fibroblasts. Cells were labeled with [^{3}H]FC (A), 20 μg/ml LDL reconstituted with [^{3}H]cholesteryl ester (CE; B), or 20 μg/ml LDL reconstituted with [^{3}H]CE and excess SM for 24 h (C). They were then loaded with 20 μg/ml cholesterol for another 24 h. After a subsequent 24 h equilibrium, cells were incubated with 10 μg/ml apoA-I for 24 h. Cholesterol efflux was determined as described in Materials and Methods. Values represent means ± SD from triplicate wells. Ctl, control.

controls in the present experiment. The results of SM and PC efflux were also expressed as absolute counts per milligram of cell protein, and no significant differences between normal and NPD-B fibroblasts were shown. Similarly, we found no significant differences in efflux when HDL_3 was used as acceptor (data not shown).

We next examined cellular cholesterol transfer by specifically targeting the lysosomal compartments with [^{3}H]CE-reconstituted LDL that entered into cells through the endocytic pathway under different labeling conditions. As shown in **Fig. 4A**, **B**, labeling with either [^{3}H]FC- or [^{3}H]CE-reconstituted LDL did not result in any significant difference in apoA-I-mediated cholesterol efflux between normal and NPD-B fibroblasts. We also investigated the effects of excess SM incorporation on the efflux ability of NPD-B fibroblasts by treating them with SM-enriched [^{3}H]CE-reconstituted LDL. As shown in Fig. 4C, additional SM loading to the lysosomes in which the SMase was defective failed to cause lipid retention in NPD-B cells. In contrast, TD fibroblasts exhibited defective cholesterol efflux under all three labeling conditions. The absence of lipid efflux defects was also observed in the commercial NPD-A and NPD-B cell lines as well as in cells from other heterozygous family members (data not shown). Interestingly, this was in agreement with the observations of Liscum, Ruggiero, and Faust (27), who showed that the LDL-cholesterol desorption rate was normal in NPD-A cells, whereas it appeared to be 3-fold slower in NPD-C cells that were defective in npc-1 protein. Because it has been suggested that the transport of LDL-cholesterol from the lysosomes to the plasma membrane is a rapid process (28), we also studied the kinetics of LDL-derived cholesterol efflux. Our time-course efflux experiments (30 min to 24 h) showed that the rate of cholesterol efflux was

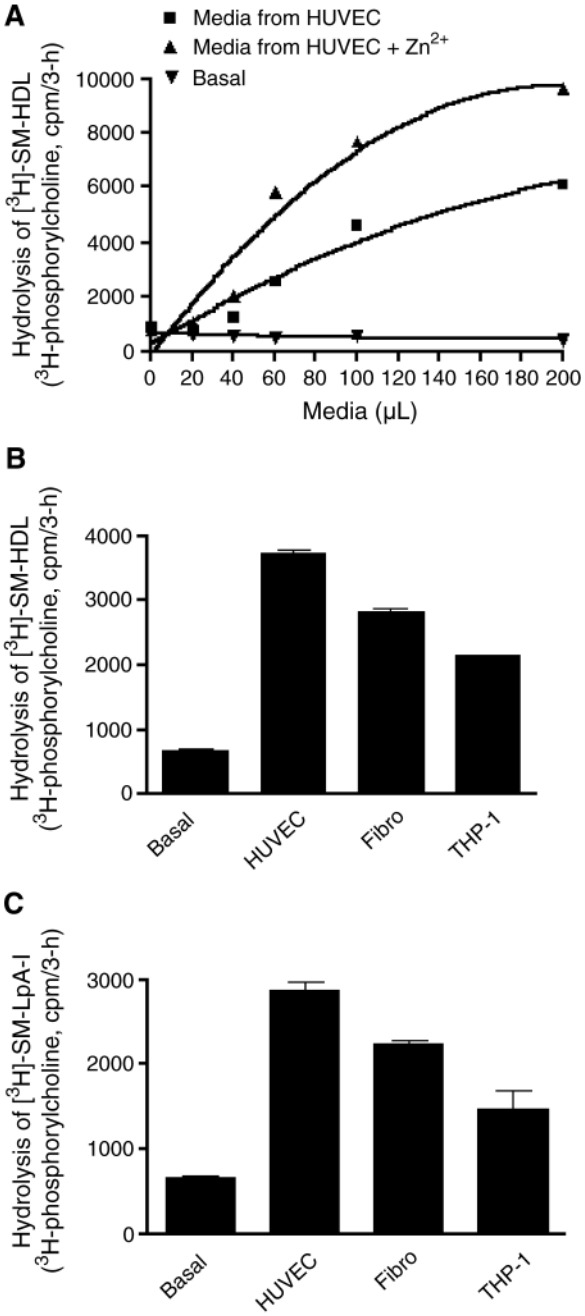

Fig. 5. Secretory sphingomyelinase (S-SMase)-mediated SM-containing HDL hydrolysis. A: [^{3}H]SM-HDL$_3$ (50 μg of protein) was incubated with increasing volumes (0–200 μl) of concentrated S-SMase-containing conditioned medium from HUVEC cells in the presence or absence of 0.1 mM $ZnCl_2$. B: [^{3}H]SM-HDL$_3$ (50 μg of protein) was incubated with 80 μl of concentrated S-SMase-containing conditioned medium from HUVEC, fibroblasts, or THP-1 in the presence of 0.1 mM $ZnCl_2$. C: [^{3}H]SM-LpA-I (20 μg of protein) was incubated with 100 μl of concentrated S-SMase-containing conditioned medium from HUVEC, fibroblasts, or THP-1 in the presence of 0.1 mM $ZnCl_2$. Basal values corresponded to [^{3}H]phosphorylcholine liberated from [^{3}H]SM in the absence of any conditioned medium. Values represent means ± SD of triplicate measures.

similar between controls and the NPD-B cell lines (data not shown). Together, our data suggested that apoA-I could mobilize cellular lipids in NPD-B cells to the plasma membrane for efflux to similar extents as in control cells. Finally, the integrity of the lipid mobilization was supported by the normal stimulation of ABCA1 expression in all patient fibroblast cell lines by LDL and 22OH/9CRA (data not shown), reflecting the fact that the imported lipids were capable of regulating ABCA1 via oxysterol (Table 2). Similarly, apoA-I binding to ABCA1 was also shown to be normal in these NPD-B cell lines (data not shown).

S-SMase mediated SM hydrolysis in HDL

Based on the observation of Tabas and colleagues (6) that different cell types secreted active S-SMase, the question was raised whether S-SMase is able to hydrolyze SM in both LpA-I and isolated plasma HDL$_3$ particles. As shown in **Fig. 5B, C**, S-SMase-containing conditioned medium collected over 24 h from HUVEC, fibroblasts, or THP-1 was able to hydrolyze the [^{3}H]SM in labeled LpA-I and HDL$_3$. We also demonstrated that increasing the volume of the conditioned medium (20–200 μl) hydrolyzed the [^{3}H]SM-HDL$_3$ in a dose-dependent manner (Fig. 5A). In contrast, the conditioned medium from NPD-B fibroblasts was not capable of hydrolyzing any [^{3}H]SM-HDL$_3$ (**Fig. 6**). To verify whether the S-SMase was secreted in the medium from NPD-B cells, we reproduced one of the mutations from our NPD-B subjects (ΔR608) by site-directed mutagenesis on the pcDNA/GS-SMPD1 expression vector and by transient transfection in CHO cells. Although its protein expression was normal, we clearly show that the ΔR608 mutant protein could not be secreted to the medium (**Fig. 7A**). Furthermore, the expressed ΔR608 mutants had abolished enzymatic activity (Fig. 7B); another mutant, Y536H, which has been described as a severe NPD-A mutation, was also created and used as a positive control. Using patient fibroblasts and HUVEC, THP-1, and CHO

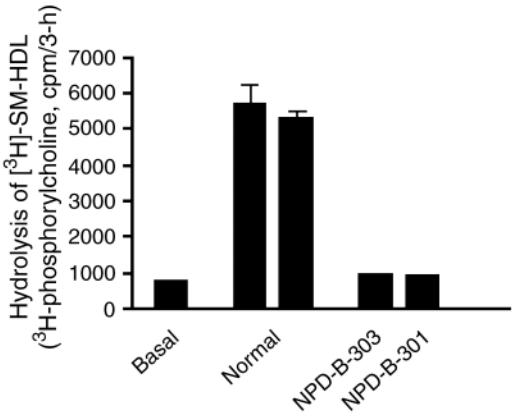

Fig. 6. Defective S-SMase-mediated SM-containing HDL hydrolysis in NPD-B. [^{3}H]SM-HDL$_3$ (65 μg of protein) was incubated with or without 120 μl of concentrated conditioned medium from normal and NPD-B fibroblasts in the presence of 0.1 mM $ZnCl_2$. Basal values corresponded to [^{3}H]phosphorylcholine liberated from [^{3}H]SM in the absence of any conditioned medium. Values represent means ± SD of triplicate measures.

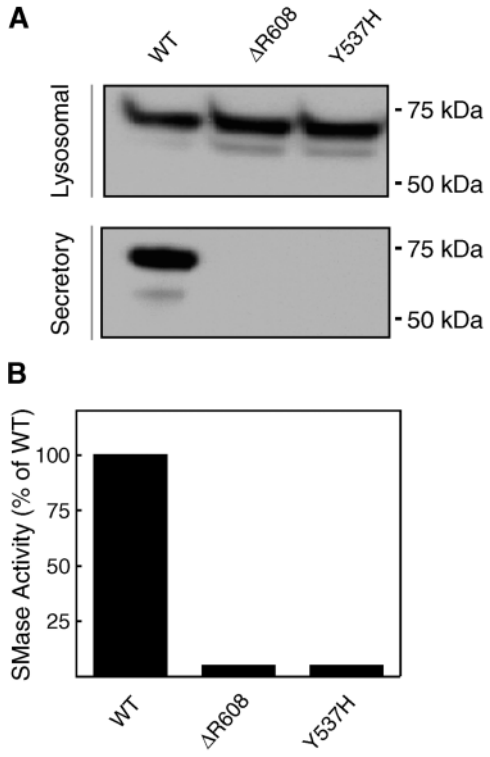

Fig. 7. Defective secretion and activity of mutant SMase (ΔR608). A: Cell lysates were harvested 24 h after transfection and prepared with lysis buffer. Conditioned medium was collected, spun at 800 *g* for 15 min to pellet any contaminating cells, and concentrated down to <1 ml using a Centriprep 30 concentrator. Cell lysates or concentrated medium were boiled in loading buffer and loaded directly on SDS-10% Tris-glycine-PAGE gels after normalization with the transfection efficiency. Gels were then electrotransferred to nitrocellulose for immunoblotting. Blots were blocked with 5% dry milk and incubated with mouse anti-V5 primary antibodies and horseradish peroxidase-conjugated rabbit anti-mouse secondary antibodies. B: SMase assay with samples generated from the overexpression system. Activity was assessed by the scintillation proximity assay. The assay mixture (100 μl) consisted of up to 40 μl of sample (cell lysates or conditioned medium), 0.1 M sodium acetate assay buffer, pH 5.0, with or without 0.1 M Zn^{2+}, and 0.625 pmol of [^{3}H]biotinylated SM substrate. The assay mixtures were incubated at 37°C for 1 h, and the reactions were stopped by the addition of streptavidin-scintillation beads. Only nonhydrolyzed [^{3}H]SM could be precipitated by the beads and detected by the β-counter. Results are expressed as percentages of wild-type (WT) values.

cell models, we provided evidence suggesting that the increased SM content of HDL in NPD-B may be attributable to defective SM hydrolysis in HDL, as a result of defects in and/or the absence of S-SMase. Our results also indirectly support the concept that S-SMase may play an important role in the modulation of SM content in lipoproteins, particularly in HDL.

DISCUSSION

Despite a growing body of information identifying SM and its derivatives as potent proatherogenic molecules (29, 30), the impact of SM on the metabolism of lipoproteins such as HDL is still poorly understood. Previous studies from our laboratory and others have reported a decreased HDL-C in NPD-A/B patients (8, 31). The cause of this decreased HDL-C, however, has never been examined. In this study, we sought to explain the association between SMPD-1 defects and low HDL-C levels.

We have demonstrated that the PL and cholesterol efflux was normal in NPD-B fibroblasts, suggesting that the cause of low HDL in NPD-B was not attributable to defective cellular lipid efflux, as seen in TD (11). Interestingly, other groups that have examined lipid efflux defects in other cell lines (such as NPD-C) have also found that NPD-A/B cells had normal efflux (27). In contrast to the clinically related disease NPD-C, in which the defects in NPC-1 transporter lead to defective cellular lipid efflux, decreased cholesterol esterification, reduced ABCA-I expression, and apoA-I binding (32), NPD-A/B fibroblasts had normal ABCA1 expression, apoA-I binding, and cholesterol esterification (data not shown).

Although lipid sequestration in NPD-A/B fibroblasts without defective lipid efflux has also been demonstrated by other laboratories (27, 33) with or without additional SM feeding, a previous study by Tabas and colleagues (34) has documented that cholesterol trafficking and efflux were impaired in acid SMase-deficient mouse macrophages. The cause of this disparity is unknown, but it may be attributable to the differences in cholesterol trafficking between fibroblasts and macrophages. Thus, one might speculate that the low plasma HDL in our NPD-B subjects could result from defective cellular cholesterol efflux from macrophages. However, the observation that ABCA1-mediated efflux from macrophages was not quantitatively important in maintaining plasma HDL levels (35, 36) did not support this possible mechanism. The relative importance of reverse cholesterol transport via macrophage ABCA1- versus non-ABCA1-mediated HDL efflux pathways with regard to HDL formation is unknown and will require further investigation. Together, our results suggest that the low plasma HDL-C level in NPD-B patients resulted from a mechanism different from that in TD patients, in whom a defect in the ABCA1 transporter leads to defective formation of HDL.

It is generally accepted that HDL catabolism is a major predictor of HDL levels (37, 38). The factors that regulate the clearance of HDL from plasma are the charge, size, and conformation of apoA-I, which are sensitive to the lipid composition of these lipoprotein particles. Indeed, it is well documented that SM inhibits the unfolding of apoA-I in discoidal and spherical reconstituted HDL and impairs the LCAT reaction (23, 24, 26). Given that NPD-B HDL particles had increased SM levels (Tables 1, 2), we examined the physiological significance of SM enrichment of HDL in the regulation of LCAT enzyme. As shown in Table 3 and Fig. 2, the increased SM content was associated with the impaired cholesterol esterification of LpA-I generated from NPD-B fibroblasts, plasma HDL from NPD-B subjects, and rLpA-I enriched with SM. This was supported by our previous finding that FC/CE ratios were significantly increased in NPD-B HDL compared with normal control subjects (8). On the basis of our observations, we suggest

that the low HDL-C observed in NPD-B was not caused by a decreased availability of lysosomally sequestered SM and cholesterol for cellular efflux onto apoA-I (Fig. 3). Rather, we propose that the abnormal SM content of their HDL impaired the function of LCAT, leading to a decrease in the CE formation necessary for HDL maturation.

At present, little is known about the origin of SM in lipoproteins. Although evidence was presented here demonstrating that both NPD-B LpA-I and plasma HDL exhibited increased SM levels, the molecular mechanism of HDL enrichment with SM has not yet been elucidated. We postulate that this SM enrichment may be attributable to increased lipid transfers from cell membranes to HDL, or, alternatively, that S-SMase activity may directly modulate the SM content in these HDL particles. In this study, we obtained evidence that supported the S-SMase hypothesis. We demonstrated that the SM content of LpA-I is sensitive to ABCA1 upregulation with 22OH/9CRA in both normal and NPD-B fibroblasts (Table 2). However, despite a significant increase of cellular SM in NPD-B cells, the efflux of both SM and cholesterol was found to be normal (Figs. 3, 4). This suggested that the increase of SM levels in NPD-B LpA-I was not a result of an increased SM mass transfer from cells via the ABCA1 pathway. One of the most unexpected findings to emerge from this study was that S-SMase from different cell types, including fibroblasts, HUVEC, and THP-1, was able to hydrolyze SM of both LpA-I and HDL (Fig. 5), underscoring the possible role of S-SMase in HDL modulation. The proposed mechanism of SMase-mediated HDL-SM hydrolysis was further strengthened by our results demonstrating that the conditioned medium from NPD-B fibroblasts failed to exhibit any HDL-SM hydrolysis (Fig. 6), consistent with our observation that mutant SMase ΔR608 exhibited defective secretion and activity (Fig. 7). It is likely that the increased SM content in HDL from NPD-B is attributable to defective S-SMase-mediated HDL-SM hydrolysis.

Our findings regarding S-SMase may have significant implications because they highlight the importance of factors operating in the extracellular space, which play a major role in the regulation of HDL concentration, composition, and subpopulation distribution. Indeed, it was documented that several lipases, including hepatic lipase, endothelial lipase, and secretory phospholipase A_2, have the ability to hydrolyze HDL PC, the major PL in HDL (39). We propose that S-SMase is another key extracellular player implicated in the hydrolysis of HDL-SM, which is the second most abundant PL in HDL. Although the mechanism by which S-SMase regulates lipoprotein metabolism requires further investigation, some pioneering biochemical studies have been performed by Tabas (7) on the proatherogenic proprieties of S-SMase. For example, Tabas (7) showed that S-SMase promotes the subendothelial aggregation and retention of LDL, leading to enhanced foam cell formation and promoting atherosclerotic vascular disease.

Earlier studies by Rothblat and colleagues (40) have documented that enrichment of HDL with PC increases cholesterol efflux, whereas its enrichment with SM decreases its influx via the scavenger receptor class B type I (SR-BI) pathway. Thus, the modification of HDL PL composition might have a large impact on both the remodeling of HDL by SR-BI and the reverse cholesterol transport process. Interestingly, de Beer and colleagues (41) have documented that HDL modification by secretory phospholipase A_2 promoted SR-BI interaction and accelerated HDL catabolism. It would be of interest to determine whether S-SMase affects the HDL/SR-BI metabolic pathway and to what extent this effect is dependent on other HDL regulatory enzymes. Finally, it is unknown whether lysosomal SMase and S-SMase deficiency may affect the hepatic and intestinal production and lipidation of apoA-I. Jiang and colleagues (21) demonstrated that increased SM content of plasma lipoproteins in apoE knockout mice led to combined production and catabolic defects and enhanced reactivity with S-SMase.

The detailed structural characteristics of nascent HDL required to transform into mature HDL are still unknown. In this study, we demonstrate that the threshold level of SM in HDL needed to inhibit the LCAT esterification is very low. This suggests that the sensitivity with which LCAT displays to nascent HDL-SM content is likely an important physiological factor for the maturation of these lipoprotein particles in vivo. This is supported by our previous studies showing that LCAT had a 2-fold greater catalytic efficiency (V_{max}/K_m) for SM-free r(HDL) compared with nascent α-LpA-I, which contained a significant amount of SM (12, 42). Thus, nascent HDL-SM content might be an important indicator of both S-SMase and LCAT efficacy.

Although indirect evidence was presented here supporting the concept that both S-SMase and LCAT might act in concert in the maturation of nascent LpA-I particles and that defective S-SMase may be responsible for the HDL deficiency in NPD-B, the roles of both SM and S-SMase in the HDL metabolic pathway in vivo are unknown at present. Undoubtedly, further elucidation of the molecular interactions between HDL and S-SMase in animal models should clarify the mechanism by which S-SMase is involved in the biogenesis and maturation of HDL particles.

This research was supported by the Canadian Institute of Health Research [Grant MOP-74703 (M.M.) and Grants MOP-15042, MOP-62834, and MT-6712 (J.G.)] and by the Heart and Stroke Foundation of Québec (J.G., M.M.). M.M. is a research scholar from the Fonds de la Recherche en Santé du Québec. The authors express their thanks to Dr. Seiji Yamaguchi (Shimane Medical University) for cordial technical advice on PL mass analysis; Dr. Yoshimitsu Kiriyama (Molecular Oncology Group, McGill University) for his very kind support; Dr. John S. Parks for kindly providing human recombinant lecithin: cholesterol acyltransferase; and Betsie Boucher for excellent technical assistance. The helpful advice of Dr Ira. Tabas is gratefully acknowledged.

REFERENCES

1. Spence, M. W., J. T. Clarke, and H. W. Cook. 1983. Pathways of sphingomyelin metabolism in cultured fibroblasts from normal and sphingomyelin lipidosis subjects. *J. Biol. Chem.* **258:** 8595–8600.

2. Silver, D. L., X. C. Jiang, T. Arai, C. Bruce, and A. R. Tall. 2000. Receptors and lipid transfer proteins in HDL metabolism. *Ann. N. Y. Acad. Sci.* **902:** 103–111.
3. Lane, J. T., P. V. Subbaiah, M. E. Otto, and J. D. Bagdade. 1991. Lipoprotein composition and HDL particle size distribution in women with non-insulin-dependent diabetes mellitus and the effects of probucol treatment. *J. Lab. Clin. Med.* **118:** 120–128.
4. Wang, N., and A. R. Tall. 2003. Regulation and mechanisms of ATP-binding cassette transporter A1-mediated cellular cholesterol efflux. *Arterioscler. Thromb. Vasc. Biol.* **23:** 1178–1184.
5. Fielding, C. J., and P. E. Fielding. 1995. Molecular physiology of reverse cholesterol transport. *J. Lipid Res.* **36:** 211–228.
6. Schissel, S. L., E. H. Schuchman, K. J. Williams, and I. Tabas. 1996. Zn^{2+}-stimulated sphingomyelinase is secreted by many cell types and is a product of the acid sphingomyelinase gene. *J. Biol. Chem.* **271:** 18431–18436.
7. Tabas, I. 1999. Secretory sphingomyelinase. *Chem. Phys. Lipids.* **102:** 123–130.
8. Lee, C. Y., L. Krimbou, J. Vincent, C. Bernard, P. Larramee, J. Genest, Jr., and M. Marcil. 2003. Compound heterozygosity at the sphingomyelin phosphodiesterase-1 (SMPD1) gene is associated with low HDL cholesterol. *Hum. Genet.* **112:** 552–562.
9. Genest, J. 2003. Lipoprotein disorders and cardiovascular risk. *J. Inherit. Metab. Dis.* **26:** 267–287.
10. Marcil, M., L. Yu, L. Krimbou, B. Boucher, J. F. Oram, J. S. Cohn, and J. Genest, Jr. 1999. Cellular cholesterol transport and efflux in fibroblasts are abnormal in subjects with familial HDL deficiency. *Arterioscler. Thromb. Vasc. Biol.* **19:** 159–169.
11. Marcil, M., R. Bissonnette, J. Vincent, L. Krimbou, and J. Genest. 2003. Cellular phospholipid and cholesterol efflux in high-density lipoprotein deficiency. *Circulation.* **107:** 1366–1371.
12. Krimbou, L., H. H. Hajj, S. Blain, S. Rashid, M. Denis, M. Marcil, and J. Genest. 2005. Biogenesis and speciation of nascent apoA-I-containing particles in various cell lines. *J. Lipid Res.* **46:** 1668–1677.
13. Jonas, A., A. Steinmetz, and L. Churgay. 1993. The number of amphipathic alpha-helical segments of apolipoproteins A-I, E, and A-IV determines the size and functional properties of their reconstituted lipoprotein particles. *J. Biol. Chem.* **268:** 1596–1602.
14. Poumay, Y., and M. F. Ronveaux-Dupal. 1985. Rapid preparative isolation of concentrated low density lipoproteins and of lipoprotein-deficient serum using vertical rotor gradient ultracentrifugation. *J. Lipid Res.* **26:** 1476–1480.
15. Roberts, D. C., N. E. Miller, S. G. Price, D. Crook, C. Cortese, A. La Ville, L. Masana, and B. Lewis. 1985. An alternative procedure for incorporating radiolabelled cholesteryl ester into human plasma lipoproteins in vitro. *Biochem. J.* **226:** 319–322.
16. Levade, T., N. Andrieu-Abadie, B. Segui, N. Auge, M. Chatelut, J. P. Jaffrezou, and R. Salvayre. 1999. Sphingomyelin-degrading pathways in human cells role in cell signalling. *Chem. Phys. Lipids.* **102:** 167–178.
17. Bartlett, G. R. 1968. Phosphorus compounds in the human erythrocyte. *Biochim. Biophys. Acta.* **156:** 221–230.
18. Lee, C. Y., A. Lesimple, A. Larsen, O. Mamer, and J. Genest. 2005. ESI-MS quantitation of increased sphingomyelin in Niemann-Pick disease type B HDL. *J. Lipid Res.* **46:** 1213–1228.
19. Parks, J. S., and A. K. Gebre. 1997. Long-chain polyunsaturated fatty acids in the sn-2 position of phosphatidylcholine decrease the stability of recombinant high density lipoprotein apolipoprotein A-I and the activation energy of the lecithin:cholesterol acyltransferase reaction. *J. Lipid Res.* **38:** 266–275.
20. Krimbou, L., M. Marcil, J. Davignon, and J. Genest, Jr. 2001. Interaction of lecithin:cholesterol acyltransferase (LCAT). alpha 2-macroglobulin complex with low density lipoprotein receptor-related protein (LRP). Evidence for an alpha 2-macroglobulin/LRP receptor-mediated system participating in LCAT clearance. *J. Biol. Chem.* **276:** 33241–33248.
21. Jeong, T., S. L. Schissel, I. Tabas, H. J. Pownall, A. R. Tall, and X. Jiang. 1998. Increased sphingomyelin content of plasma lipoproteins in apolipoprotein E knockout mice reflects combined production and catabolic defects and enhances reactivity with mammalian sphingomyelinase. *J. Clin. Invest.* **101:** 905–912.
22. Haidar, B., M. Denis, M. Marcil, L. Krimbou, and J. Genest, Jr. 2004. Apolipoprotein A-I activates cellular cAMP signaling through the ABCA1 transporter. *J. Biol. Chem.* **279:** 9963–9969.
23. Rye, K. A., N. J. Hime, and P. J. Barter. 1996. The influence of sphingomyelin on the structure and function of reconstituted high density lipoproteins. *J. Biol. Chem.* **271:** 4243–4250.
24. Bolin, D. J., and A. Jonas. 1996. Sphingomyelin inhibits the lecithin-cholesterol acyltransferase reaction with reconstituted high density lipoproteins by decreasing enzyme binding. *J. Biol. Chem.* **271:** 19152–19158.
25. Subbaiah, P. V., and H. Monshizadegan. 1988. Substrate specificity of human plasma lecithin-cholesterol acyltransferase towards molecular species of phosphatidylcholine in native plasma. *Biochim. Biophys. Acta.* **963:** 445–455.
26. Subbaiah, P. V., and M. Liu. 1993. Role of sphingomyelin in the regulation of cholesterol esterification in the plasma lipoproteins. Inhibition of lecithin-cholesterol acyltransferase reaction. *J. Biol. Chem.* **268:** 20156–20163.
27. Liscum, L., R. M. Ruggiero, and J. R. Faust. 1989. The intracellular transport of low density lipoprotein-derived cholesterol is defective in Niemann-Pick type C fibroblasts. *J. Cell Biol.* **108:** 1625–1636.
28. Brasaemle, D. L., and A. D. Attie. 1990. Rapid intracellular transport of LDL-derived cholesterol to the plasma membrane in cultured fibroblasts. *J. Lipid Res.* **31:** 103–112.
29. Jiang, X. C., F. Paultre, T. A. Pearson, R. G. Reed, C. K. Francis, M. Lin, L. Berglund, and A. R. Tall. 2000. Plasma sphingomyelin level as a risk factor for coronary artery disease. *Arterioscler. Thromb. Vasc. Biol.* **20:** 2614–2618.
30. Tabas, I. 2004. Sphingolipids and atherosclerosis. A mechanistic connection? A therapeutic opportunity? *Circulation.* **110:** 3400–3401.
31. McGovern, M. M., T. Pohl-Worgall, R. J. Deckelbaum, W. Simpson, D. Mendelson, R. J. Desnick, E. H. Schuchman, and M. P. Wasserstein. 2004. Lipid abnormalities in children with types A and B Niemann Pick disease. *J. Pediatr.* **145:** 77–81.
32. Choi, H. Y., B. Karten, T. Chan, J. E. Vance, W. L. Greer, R. A. Heidenreich, W. S. Garver, and G. A. Francis. 2003. Impaired ABCA1-dependent lipid efflux and hypoalphalipoproteinemia in human Niemann-Pick type C disease. *J. Biol. Chem.* **278:** 32569–32577.
33. Pentchev, P. G., M. E. Comly, H. S. Kruth, M. T. Vanier, D. A. Wenger, S. Patel, and R. O. Brady. 1985. A defect in cholesterol esterification in Niemann-Pick disease (type C) patients. *Proc. Natl. Acad. Sci. USA.* **82:** 8247–8251.
34. Leventhal, A. R., W. Chen, A. R. Tall, and I. Tabas. 2001. Acid sphingomyelinase-deficient macrophages have defective cholesterol trafficking and efflux. *J. Biol. Chem.* **276:** 44976–44983.
35. Aiello, R. J., D. Brees, P. A. Bourassa, L. Royer, S. Lindsey, T. Coskran, M. Haghpassand, and O. L. Francone. 2002. Increased atherosclerosis in hyperlipidemic mice with inactivation of ABCA1 in macrophages. *Arterioscler. Thromb. Vasc. Biol.* **22:** 630–637.
36. Haghpassand, M., P. A. Bourassa, O. L. Francone, and R. J. Aiello. 2001. Monocyte/macrophage expression of ABCA1 has minimal contribution to plasma HDL levels. *J. Clin. Invest.* **108:** 1315–1320.
37. Rader, D. J., and C. Maugeais. 2000. Genes influencing HDL metabolism: new perspectives and implications for atherosclerosis prevention. *Mol. Med. Today.* **6:** 170–175.
38. Tall, A. R., X. Jiang, Y. Luo, and D. Silver. 2000. 1999 George Lyman Duff Memorial Lecture. Lipid transfer proteins, HDL metabolism, and atherogenesis. *Arterioscler. Thromb. Vasc. Biol.* **20:** 1185–1188.
39. Rader, D. J., and K. A. Dugi. 2000. The endothelium and lipoproteins: insights from recent cell biology and animal studies. *Semin. Thromb. Hemost.* **26:** 521–528.
40. Yancey, P. G., M. Llera-Moya, S. Swarnakar, P. Monzo, S. M. Klein, M. A. Connelly, W. J. Johnson, D. L. Williams, and G. H. Rothblat. 2000. High density lipoprotein phospholipid composition is a major determinant of the bi-directional flux and net movement of cellular free cholesterol mediated by scavenger receptor BI. *J. Biol. Chem.* **275:** 36596–36604.
41. de Beer, F. C., P. M. Connell, J. Yu, M. C. de Beer, N. R. Webb, and D. R. van der Westhuyzen. 2000. HDL modification by secretory phospholipase A(2) promotes scavenger receptor class B type I interaction and accelerates HDL catabolism. *J. Lipid Res.* **41:** 1849–1857.
42. Denis, M., B. Haidar, M. Marcil, M. Bouvier, L. Krimbou, and J. Genest, Jr. 2004. Molecular and cellular physiology of apolipoprotein A-I lipidation by the ATP-binding cassette transporter A1 (ABCA1). *J. Biol. Chem.* **279:** 7384–7394.